# Raman spectrum study of graphite irradiated by swift heavy ions*

Zhai Peng-Fei(翟鹏飞)[a], Liu Jie(刘 杰)[a)†], Zeng Jian(曾 健)[a)b)c)], Yao Hui-Jun(姚会军)[a)], Duan Jing-Lai(段敬来)[a)], Hou Ming-Dong(侯明东)[a)], Sun You-Mei(孙友梅)[a)], and Ewing Rodney Charles[d)]

[a)] *Institute of Modern Physics, Chinese Academy of Sciences, Lanzhou* 730000, *China*
[b)] *University of Chinese Academy of Sciences, Beijing* 100049, *China*
[c)] *School of Nuclear Science and Technology, Lanzhou University, Lanzhou* 730000, *China*
[d)] *Department of Geological and Environmental Sciences, Stanford University, Stanford, CA* 94305-2115, *USA*

(Received 26 March 2014; revised manuscript received 27 June 2014; published online 10 October 2014)

Highly oriented pyrolytic graphites are irradiated with 40.5-MeV and 67.7-MeV $^{112}$Sn-ions in a wide range of fluences: $1\times10^{11}$ ions/cm$^2$–$1\times10^{14}$ ions/cm$^2$. Raman spectra in the region between 1200 cm$^{-1}$ and 3500 cm$^{-1}$ show that the disorder induced by Sn-ions increases with ion fluence increasing. However, for the same fluence, the amount of disorder is greater for 40.5-MeV Sn-ions than that observed for 67.7-MeV Sn-ions, even though the latter has a slightly higher value for electronic energy loss. This is explained by the ion velocity effect. Importantly, $\sim$ 3-cm$^{-1}$ frequency shift toward lower wavenumber for the *D* band and $\sim$ 6-cm$^{-1}$ shift toward lower wavenumber for the 2*D* band are observed at a fluence of $1\times10^{14}$ ions/cm$^2$, which is consistent with the scenario of radiation-induced strain. The strain formation is interpreted in the context of inelastic thermal spike model, and the change of the 2*D* band shape at high ion fluence is explained by the accumulation of stacking faults of the graphene layers activated by radiation-induced strain around ion tracks. Moreover, the hexagonal structure around the ion tracks is observed by scanning tunneling microscopy, which confirms that the strains near the ion tracks locally cause electronic decoupling of neighboring graphene layers.

**Keywords:** Raman spectroscopy, swift heavy ions, highly oriented pyrolytic graphite, strain, ion velocity effect

**PACS:** 61.82.–d, 61.72.Ff, 61.72.Hh **DOI:** 10.1088/1674-1056/23/12/126105

## 1. Introduction

Ion irradiation and implantation of graphite have been performed for many years,[1–7] in order to investigate the changes in the properties of graphite used as a moderator or shielding material in a nuclear reactor. Recently, the use of graphite as a target in fragment separators in high-energy high-intensity beam facilities has aroused the interest in graphite interactions with high-energy ions. Upon ion irradiation, structural change has been observed in graphite. As an example, nanodiamond crystallites form in highly oriented pyrolytic graphite (HOPG) irradiated by swift monoatomic ions and $C_{60}$ clusters as observed using transmission electron microscope (TEM).[3] Scanning tunneling microscopy (STM) measurements display that hillocks are created by MeV–GeV heavy ions on the HOPG surface which have a mean diameter of 2.5 nm and an average height of less than 1 nm.[4] Furthermore, TEM images show that the ion track in HOPG is surrounded by a strain halo within the otherwise undisturbed material,[7] and the tracks consist of a discontinuous sequence of perturbed zones.[3,4] The "ion velocity effect", i.e., for a given value of electronic energy loss ($S_e$), the irradiation-induced damage is more severe for low-velocity ions compared with for high-velocity ions, was first observed in ion-irradiated yttrium garnet $Y_3Fe_5O_{12}$.[8] So far, this so-called ion velocity effect has been reported in many materials.[9–11] Qualitatively, the ion velocity effect can be understood in the context of the energy deposited density.[8,12] Still, there are very few studies of this effect in HOPG.[13]

Raman spectroscopy is a commonly used technique for studying the structures of carbon materials. It can provide valuable information about defects, the sizes of crystallites in- and out-plane of graphite, edge states, and stacking of the graphene layers,[14–17] even distinguishing between mono-layer graphene and multi-layer graphene.[18] In previous studies, the first-order Raman spectrum of ion-irradiation graphite was investigated extensively.[1,2,5,6,12] Because it is easy to know the extent of disorder in the basal plane of graphite induced by ion irradiation using Tuinstra–Koenig equation.[19] However, there have been few studies that deal with the second-order Raman spectra of ion-irradiation or ion-implantation graphite.

In this work, we investigate first- and second-order Raman spectra observed for HOPG irradiated with Sn-ions, in a wide fluence range from $1\times10^{11}$ ions/cm$^2$ to $1\times10^{14}$ ions/cm$^2$ with the energies of 40.5 MeV and 67.7 MeV respectively. The in-plane crystallite size, $L_\alpha$, is deduced from the integrated in-

*Project supported by the National Natural Science Foundation of China (Grant Nos. 11179003, 10975164, 10805062, and 11005134).
†Corresponding author. E-mail: j.liu@impcas.ac.cn
© 2014 Chinese Physical Society and IOP Publishing Ltd 

tensity ratio $I_D/I_G$ between the $D$ and $G$ bands by using a general empirical formula deduced by Cançado *et al.*[15] The ion velocity effect in HOPG is observed and discussed by comparing the two Raman spectra of HOPG irradiated respectively with 40.5-MeV and 67.7-MeV Sn-ions. Another main focus is to study the evolutions of the $D$ and $2D$ bands with increasing the ion fluence. The $2D$ band shape changes of the Raman spectra observed in HOPG after high ion fluence irradiation are explained.

## 2. Experiment

HOPG samples (Advanced Ceramics Co., Grade ZYB) were first cleaved several times using a common adhesive tape to obtain a fresh basal plane. Then the samples were irradiated by scanning $^{112}$Sn-ions with an initial kinetic energy of 3.7 MeV/u in Heavy Ion Research Facility in Lanzhou (HIRFL). The energy of beam was reduced to 2.24 MeV/u because the ions first passed through a 10-μm aluminum foil that served as an on-line fluence control, which had been calibrated using a Faraday cup. The aluminum foils (the purity is 99.99%) with thickness values of 13.8 μm and 16.9 μm, were used as degraders. The irradiation experiments were carried out at normal incidence (with respect to the basal plane of graphite) under room temperature. The ion flux was limited to $\sim 5$–$8\times10^8$ ions/cm$^2$·s to avoid macroscopic sample heating, with a "beam distribution based on time" mode, i.e., 30 s was a period wherein 20 s is beam time and 10 s is empty. Fluence series covered values from $1\times10^{11}$ ions/cm$^2$ up to $1\times10^{14}$ ions/cm$^2$. The irradiation parameters are listed in Table 1. The energy and energy dispersion were calculated using the SRIM03 code.[20]

**Table 1.** Irradiation parameters for HOPG. $S_e$ denotes the electronic energy loss calculated with the SRIM 03 code.[20] Ion relative velocity $\beta = v/c$, where $v$ and $c$ are the ion velocity and light velocity, respectively.

| Ion | Energy/MeV | Degrader/μm | Energy dispersion/MeV | $S_e$/(keV/nm) | Relative velocity ($\beta = v/c$) | Range/μm |
|---|---|---|---|---|---|---|
| $^{112}$Sn | 67.7 | 13.8 | 3.2 | 11.7 | 0.036 | 10 |
| | 40.5 | 16.9 | 4.5 | 9.6 | 0.028 | 7 |

After irradiation experiment, LabRAM HR800 Raman spectrometer (Jobin Yvon Co.) was used to analyze the irradiated HOPG samples in 180° geometry at room temperature. The excitation wavelength is 532.2 nm and the optical skin depth in HOPG is about 50 nm. A 50× objective lens was used to obtain a laser beam diameter of about 2 μm. The measurement time for each sample was 3 minutes. Each sample was characterized at three different positions. The Stokes scattering was analyzed with about 0.5-cm$^{-1}$ spectral resolution using an 1800-lines mm$^{-1}$ grating. Intensities, positions, and widths were deduced by fitting Lorentzian functions to the bands. The projected ranges in HOPG are 7 μm and 10 μm for 40.5-MeV and 67.7-MeV Sn-ions respectively. They are much longer than the optical skin depth of 532.2-nm laser in HOPG. Thus, the correction procedure as given in Refs. [2] and [21] was not needed. The ion tracks on the surface were characterized by STM (Multimode 8, Bruker Co.) in constant current mode.

## 3. Results and discussion

Figure 1 shows typical first- and second-order Raman spectra of HOPG samples subjected to irradiations of 40.5-MeV and 67.7-MeV Sn-ions with fluences ranging from $1\times10^{11}$ ions/cm$^2$ to $1\times10^{14}$ ions/cm$^2$, respectively. The most prominent feature in the Raman spectra of HOPG is the so-called $G$ band appearing at 1580 cm$^{-1}$. The $G$ band is a doubly degenerate (iTO and LO) phonon mode ($E_{2g}$ symmetry) at the Brillouin zone center which is Raman active for sp$^2$ carbon networks.[22] The full width at half-maximum of the $G$ band increases from 14.1 cm$^{-1}$ for pristine HOPG to 23.1 cm$^{-1}$ for the irradiated HOPG at a fluence of $1\times10^{14}$ ions/cm$^2$, while just a slight shift ($\sim 0.7$ cm$^{-1}$) of the $G$ band to lower wavenumber is observed.

The $D$ band at $\sim 1363$ cm$^{-1}$ is observed after low ion fluence irradiation. The $D$ peak is due to the breathing mode of six-atom ring and requires a defect for its activation.[22] With the increase of the ion fluence, the $D'$ band appears at $\sim 1623$ cm$^{-1}$. They are dispersive in frequency because of a double resonance process.[23] In Fig. 2, the $D$ band is shown as a function of ion fluence. The position of the $D$ band remains fixed up to a fluence of $6.3\times10^{13}$ ions/cm$^2$. The intensity of the $D$ band increases with ion fluence increasing. The integrated intensity ratio $I_D/I_G$ between the $D$ and $G$ bands is shown in Fig. 3. Note that at the same fluence, $I_D/I_G$ for irradiated HOPG with ion energy 67.7 MeV is always lower than that with 40.5 MeV, although the former has a bit higher $S_e$. This is explained by the ion velocity effect.[13] The in-plane crystalline size, $L_a$, deduced from the formula[15] ($\lambda_L$ is the wavelength of the laser) is also plotted in Fig. 3.

$$L_a = \left(2.4 \times 10^{-10}\right) \lambda_L^4 \left(I_D/I_G\right)^{-1}, \quad (1)$$

$L_a$ is also considered to be equal to the in-plane phonon correlation length.[2,21] Furthermore, it corresponds to the mean distance between defects,[2,21] $L_D$, which is given as

$$L_D = 1/\sqrt{\eta \Phi}, \quad (2)$$

where $\eta$ is the ion track creation yield and $\Phi$ is the ion fluence. If $\eta = 1$, i.e., one ion creates one corresponding ion track, the discrepancy between $L_a$ and $L_D$ will be significant ($L_a \gg L_D$).[5,13] So, it is logical to assume that the ion track creation yield is $\eta < 1$ in HOPG irradiated with swift heavy ions. An alternative explanation is that $L_a$ deduced from the equation represents the mean value within the optical skin depth ($\sim 50$ nm for 532.2-nm excitation wavelength in graphite), wherein the formation of ion track inside the bulk is markedly suppressed as compared with in the surface due to the strong recrystallization process inside the monatomic material,[4] consequently making the statistical value of $L_a$ larger. In fact, both of these explanations have been proven to be correct.[3,4] According to the above perspectives, the phenomena shown in Fig. 3, i.e., $L_a$ for 40.5-MeV ion irradiation is always lower than for 67.7 MeV, can be explained as the 40.5-MeV Sn-ions inducing a higher ion track creation yield or/and ion tracks with more limited degree of discontinuity in HOPG due to the ion velocity effect.[3,12,13]

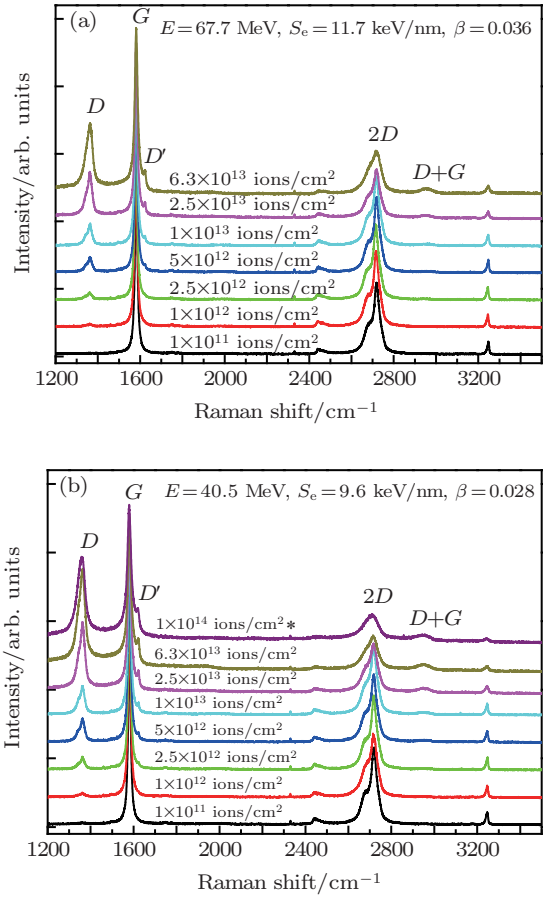



**Fig. 1.** (color online) First- and second-order Raman spectra of HOPG irradiated with (a) 67.7-MeV and (b) 40.5-MeV Sn-ions at different fluences. The peak indicated by the asterisk comes from the Raman mode of $N_2$ gas ($\sim 2330$ cm$^{-1}$) presented in the air surrounding the samples,[14] which remains fixed as observed, indicating the red shift of the $D$ and $2D$ bands at a fluence of $1\times10^{14}$ ions/cm$^2$ not due to the calibration error.

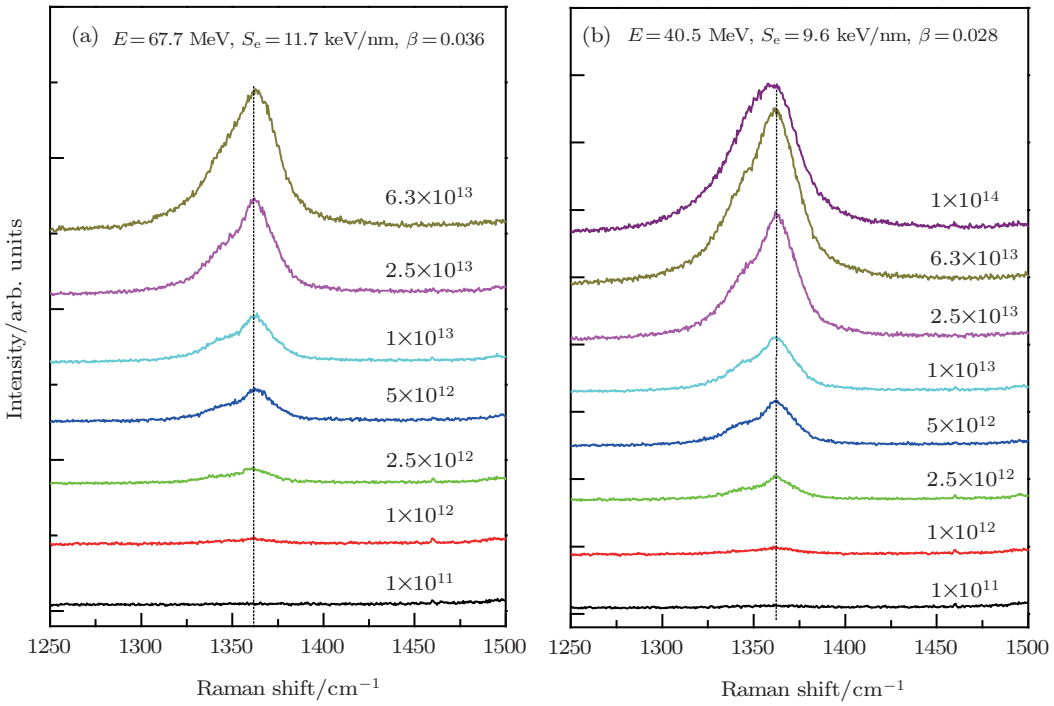



**Fig. 2.** (color online) The $D$ band of Raman spectra of HOPG irradiated with (a) 67.7-MeV and (b) 40.5-MeV Sn-ions at different fluences.

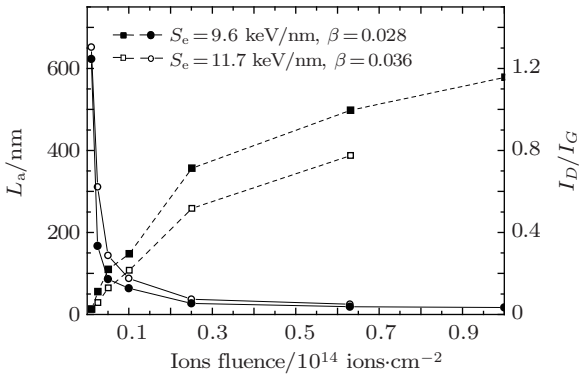



**Fig. 3.** The variations of intensity ratio $I_D/I_G$ (square) for the $D$ and $G$ bands, and the in-plane crystallite size $L_a$ (circle) deduced from the formula $L_a = (2.4 \times 10^{-10})\,\lambda_L^4\,(I_D/I_G)^{-1}$,[15] as a function with ion fluence.

As ion fluence exceeds $5\times10^{12}$ ions/cm$^2$, a new peak appears at about 2950 cm$^{-1}$. This is due to the combination mode of $D$ and $G$ modes. It is also induced by disorder, which has been observed in basal and edge plane of pyrolytic graphite, nano-graphite, and glassy carbon.[24,25] At a fluence of $6.3\times10^{13}$ ions/cm$^2$, the change of the 2$D$ band shape (at $\sim$ 2700 cm$^{-1}$) is observed (see Figs. 1 and 4). Note that in Figs. 2 and 4, $\sim$ 3-cm$^{-1}$ shift toward lower wavenumber for the $D$ band and $\sim$ 6-cm$^{-1}$ shift toward lower wavenumber for the 2$D$ band occur at the highest fluence ($1\times10^{14}$ ions/cm$^2$). The shift of the Raman peak indicates the buildup of strain.[26,27] Meanwhile, more evident is the change in the 2$D$ band shape (Fig. 4). The integrated intensity ratio of the $2D_1$ peak to $2D_2$ peak varies from 0.44 at the $1\times10^{11}$ ions/cm$^2$ to 1.67 at $1\times10^{14}$ ions/cm$^2$. Strains around the ion tracks in HOPG and GeS induced by swift heavy ions have been observed by high-resolution transmission electron spectroscope.[7,28] The strain formation in irradiated HOPG can be explained in the context of the inelastic thermal spike model.[12] In this model, the ion energy is first deposited on the electrons and then transferred to the atomic subsystem of graphite through the electron–phonon interaction. Consequently, the temperature of the graphite (2.26 g/cm$^3$ for ideal solid phase) reaches and even exceeds the melting point, then begins to expand towards the density of liquid carbon (1.6 g/cm$^3$[29]). When this occurs, pressure increases at the boundary between the liquid (the ion track area) and solid (the undisturbed area around the ion track) phases of the graphite, creating a strain wave.[30,31] Thus, the presence of strain in the irradiated HOPG can be detected by Raman spectroscopy, as long as it accumulates with ion fluence increasing.

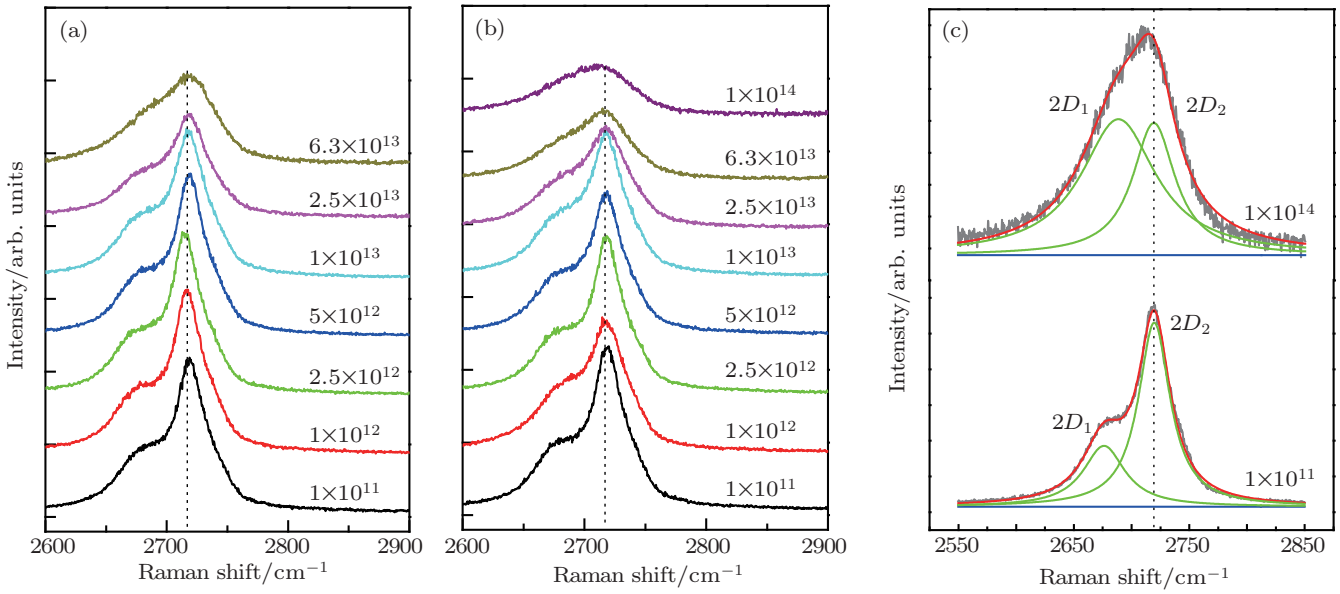



**Fig. 4.** (color online) The 2$D$ band of Raman spectra of HOPG irradiated with (a) 67.7-MeV and (b) 40.5-MeV Sn-ions at different fluences. Panel (c) displays the fitting results to the 2$D$ band at the fluences of $1\times10^{11}$ ions/cm$^2$ and $1\times10^{14}$ ions/cm$^2$ for the 40.5-MeV Sn-ions, respectively.

The shape of the 2$D$ band is related to the stacking manner of the graphitic material.[14,16,18] In particular, the Raman spectrum of turbostratic graphite (without the planar AB stacking) shows a symmetrical peak of 2$D$ band because of the very weak interaction between the adjacent graphene layers.[16,18,32] Thus, it is assumed that the strain around the ion tracks in graphite affects the interlayer separation ($> 0.335$ nm) of the undisturbed structure nearby and decouples the interaction of the adjacent layers. As the density of stacking faults around the ion tracks increases with ion fluence increasing, there is an increasingly evident change in the 2$D$ band shape.

In most cases, STM images of graphite show a triangular structure in atomic resolution, where only half of the carbon atoms are actually visualized. This phenomenon is attributed to the difference in the local density of states, specifically to graphite, determined by the interlayer interaction and the structural nonequivalence of the atomic positions.[33,34] Considering this reason, it can be predicted that when a monolayer grapheme is characterized, the honeycomb structure will be observed. Indeed, this hypothesis has been confirmed by Stolyarova *et al.*[35] Recently, Wong *et al.*[36] demonstrated that the STM tip can be used to modify the spacing between the graphene layers locally due to the attractive forces between the tip and graphite sample. It can essentially decouple the top layer, thus creating graphene locally. Consequently, the hexagonal symmetry can be visualized by STM. Figure 5 shows an STM image of irradiated HOPG by 40.5-MeV Sn-ions. The hexagonal structure around the ion tracks is clearly seen, whereas, in the lower part of the image is the triangular structure, which is far away from the ion tracks. It is assumed that the strain around the tracks induced by ion irradiation acts like the attractive forces between the STM tip and sample,[36] thus locally affecting the interlayer separation and decoupling the interaction of the top and lower layer of graphite. It should be mentioned that due to the stochastic nature of the linear energy transfer,[4] the extent of the strain around the ion tracks also has stochastic nature. So, it is reasonable that not each of ion tracks around with enough force (strain) happens to decouple the top graphene layer from the underlying layers.

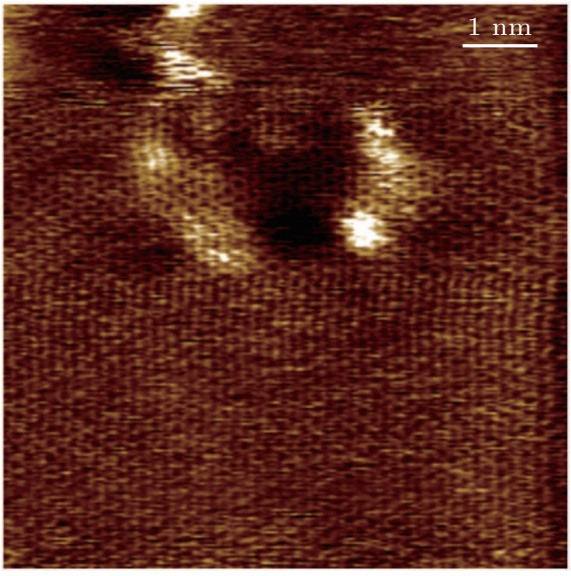



**Fig. 5.** (color online) High-resolution STM image of HOPG surface irradiated with 40.5-MeV Sn-ions obtained in constant current mode. The hexagonal structure of the graphite around the ion tracks is visualized.

## 4. Conclusion

HOPG surfaces are irradiated with 40.5-MeV and 67.7-MeV, respectively, Sn-ions over a range of fluences: $1\times10^{11}$ ions/cm$^2$ to $1\times10^{14}$ ions/cm$^2$. First- and second-order Raman spectra of the irradiated HOPG show that the ion velocity effect plays an important role in ion track formation. More importantly, the irradiation-induced strains around the tracks are observed as downshifts of the $D$ and $2D$ bands at the highest fluence. The formation of the strain around the ion tracks is interpreted in the context of inelastic thermal spike model. Meanwhile, the change of the $2D$ band shape is explained in the terms of the formation of stacking faults of the graphene layers. This hypothesis is confirmed by the STM measurements. Thus, Raman spectrum provides comprehensive information about the features of swift heavy ion tracks in HOPG, such as the discontinuity of the ion tracks, the existence of the strain around the ion tracks, the interlayer separation change of the undisturbed structure induced by the strain around the ion tracks.

## References


[1] Elman B S, Shayegan M, Dresselhaus M S, Mazurek H and Dresselhaus G 1982 *Phys. Rev. B* **25** 4142

[2] Nakamura K and Kitajima M 1992 *Phys. Rev. B* **45** 78

[3] Dunlop A, Jaskierowicz G, Ossi P M and Della-Negra S 2007 *Phys. Rev. B* **76** 155403

[4] Liu J, Neumann R, Trautmann C and Müller C 2001 *Phys. Rev. B* **64** 184115

[5] Liu J, Hou M D, Trautmann C, Neumann R, Müller C, Wang Z G, Zhang Q X, Sun Y M, Jin Y F, Liu H W and Gao H J 2003 *Nucl. Instrum. Method B* **212** 303

[6] Fu Y C, Jin Y F, Yao C F and Zhang C H 2009 *Chin. Phys. Lett.* **26** 016101

[7] Glasmacher U A, Lang M, Keppler H, Langenhorst F, Neumann R, Schardt D, Trautmann C and Wagner G A 2006 *Phys. Rev. Lett.* **96** 195701

[8] Meftah A, Brisard F, Costatini J M, Hage-Ali M, Stoquert J P, Studer F and Toulemonde M 1993 *Phys. Rev. B* **48** 920

[9] Gaiduk P I, Larsen A N, Hansen J L, Trautmann C and Toulemonde M 2003 *Appl. Phys. Lett.* **83** 1746

[10] Wang Z G, Dufour Ch, Cabeau B, Dural J, Fuchs G, Paumier E, Pawlak F and Toulemonde M 1996 *Nucl. Instrum. Method B* **107** 175

[11] Ishikawa N, Iwase A, Chimi Y, Michikami O, Wakana H, Hashimoto T, Kambara T, Müller C and Neumann R 2002 *Nucl. Instrum. Method B* **193** 278

[12] Toulemonde M, Trautmann C, Balanzat E, Hjort K and Weidinger A 2004 *Nucl. Instrum. Method B* **216** 1

[13] Zhai P F, Liu J, Duan J L, Chang H L, Zeng J, Hou M D and Sun Y M 2011 *Nucl. Instrum. Method B* **269** 2035

[14] Pimenta M A, Dresselhaus G, Dresselhaus M S, Cancçado L G, Jorio A and Saito R 2007 *Phys. Chem. Chem. Phys.* **9** 1276

[15] Cançado L G, Takai K, Enoki T, Endo M, Kim Y A, Mizusaki H, Jorio A, Coelho L N, Magalhaes-Paniago R and Pimenta M A 2006 *Appl. Phys. Lett.* **88** 163106

[16] Cançado L G, Takai K, Enoki T, Endo M, Kim Y A, Mizusaki H, Speziali N L, Jorio A and Pimenta M A 2008 *Carbon* **46** 272

[17] Cançado L G, Pimenta M A, Neves B R A, Dantas M S S and Jorio A 2004 *Phys. Rev. Lett.* **93** 247401

[18] Ferrari A C, Meyer J C, Scardaci V, Casiraghi C, Lazzeri M, Mauri F, Piscanec S, Jiang D, Novoselov K S, Roth S and Geim A K 2006 *Phys. Rev. Lett.* **97** 187401

[19] Tuinstra F and Koenig J L 1970 *J. Chem. Phys.* **53** 1126

[20] Ziegler J F 2004 *Nucl. Instrum. Method B* **219–220** 1027

[21] Asari E, Kamioka I, Nakamura K G, Kawabe T, Lewis W A and Kitajima M 1994 *Phys. Rev. B* **49** 1011

[22] Ferrari A C and Basko D M 2013 *Nat. Nanotech.* **8** 235

[23] Thomsen C and Reich S 2000 *Phys. Rev. Lett.* **85** 5214

[24] Neumanich R J and Solin S A 1979 *Phys. Rev. B* **20** 392

[25] Kawashima Y and Katagiri G 1995 *Phys. Rev. B* **52** 10053

[26] Mohiuddin T M G, Lombardo A, Nair R R, Bonetti A, Savini G, Jalil R, Bonini N, Basko D M, Galiotis C, Marzari N, Novoselov K S, Geim A K and Ferrari A C 2009 *Phys. Rev. B* **79** 205433

[27] del Corro E, Taravillo M and Baonza V G 2012 *Phys. Rev. B* **85** 033407

[28] Vetter J, Scholz R, Dobrev D and Nistor L 1998 *Nucl. Instrum. Method B* **141** 747

[29] Steinbeck J, Dresselhaus G and Dresselhaus M S 1990 *Int. J. Thermophys.* **11** 789

[30] Enquist H, Navirian H, Hansen T N, Lindenberg A M, Sondhauss P, Synnergren O, Wark J S and Larsson J 2007 *Phys. Rev. Lett.* **98** 225502

[31] Nüske R, Jurgilaitis A, Enquist H, Harb M, Fang Y, Hakanson U and Larsson J 2012 *Appl. Phys. Lett.* **100** 043102

[32] Lespade P, Marchand A, Couzi M and Cruege F 1984 *Carbon* **22** 375

[33] Tomanek D and Louie S G 1988 *Phys. Rev. B* **37** 8327

[34] Tomanek D, Louie S G, Mamin H J, Abraham D W, Thomson R E, Ganz E and Clarke J 1987 *Phys. Rev. B* **35** 7790

[35] Stolyarova E, Rim K T, Ryu S, Maultzsch J, Kim P, Brus L E, Heinz T F, Hybertsen M S and Flynn G W 2007 *Proc. Natl. Acad. Sci. USA* **104** 9209

[36] Wong H S, Durkan C and Chandrasekhar N 2009 *ACS Nano* **3** 3455